Hydrodynamic evaluation of a new dispersive aortic cannula (Stealthflow)

（新しい分散型大動脈カニューレ（ステルスフロー）の流動特性解析）

申 請 者　　弘前大学大学院医学研究科
循環病態科学領域心臓血管外科学教育研究分野
氏　　名　　後　藤　　武
指導教授　　福　田　　幾　夫

Abstract

The aim of this study was to evaluate flow from a new dispersive aortic cannula (Stealthflow) in the aortic arch using flow visualization methods. Particle image velocimetry was used to analyze flow dynamics in the mock aortic model. Flow patterns, velocity distribution, and streamlines with different shape cannulas were evaluated in a glass aortic arch model. We compared flow parameters in two different dispersive type cannulas: the Stealthflow and the Soft-flow cannula. A large vortex and regurgitant flow were observed in the aortic arch with both cannulas. With the Stealthflow cannula, a high-velocity area with a maximum velocity of 0.68 m/s appeared on the ostium of the cannula in the longitudinal plane. With the Soft-flow cannula, ‘multiple jet streams, each with a velocity less than 0.60 m/s, were observed at the cannula outlet. Regurgitant flow from the cannula to the brachiocephalic artery and to the ascending aorta on the greater curvature was specific to the Soft-flow cannula. The degree of regurgitation on the same site was lower with the Stealthflow cannula than with the Soft-flow cannula. The Stealthflow cannula has similar flow properties to those of the Soft-flow cannula according to glass aortic model analysis. It generates gentle flow in the aortic arch and slow flow around the ostia of the aortic arch vessels. The Stealthflow cannula is as effective as the

Soft-flow cannula. Care must be taken when the patient has thick atheromatous plaque or frail atheroma on the lesser curvature of the aortic arch.

Background

Cerebral injury in open-heart surgery is an uncommon complication. However, once it occurs, it is a significant cause of disability and death. There are many causes of cerebral injury, including brain hypoperfusion due to perioperative hypotension, occlusive lesion of the carotid vertebral system, postoperative cardiac arrest, air-embolism, fat-embolism, and atheroembolism. Age and prolonged cardiopulmonary bypass (CPB) and the presence of carotid and peripheral vascular disease strongly affect the incidence of stroke after heart surgery. Atheroembolism from a diseased ascending aorta is an emerging problem, because elderly patients have a high prevalence of an atherosclerotic aorta. Manipulation of the diseased aorta induces detachment of the atheromatous debris from the aortic cannulation site or aortic clamp. Another mechanism of atheroembolism is the ‘‘sandblast effect’’ of the jet flow from the aortic perfusion site. We previously described the effect of jet flow to the normal and diseased aorta in mock aortic

models. We demonstrated that dispersive cannulas were better than an end-hole cannula from the viewpoint of the sandblast effect and regurgitant flow from the distal aortic arch to arch vessels [1]. The Stealthflow cannula$^{\grave{O}}$ (Toyobo, Osaka, Japan) was developed to attenuate flow and for easy handling. The aim of this study was to evaluate flow from the Stealthflow cannula in the aortic arch using flow visualization methods.

Methods

Experimental designs

Aortic arch model

We reconstructed glass aortic models from contrast-enhanced computed tomography scan images of patients who did not have cardiovascular disease (Fig. 1). This transparent glass thoracic aortic model included the ascending aorta, the transverse aortic arch, the arch vessels, and the descending aorta. This glass model regenerated the three- dimensional geometry of the aortic arch with the twisting and curvature of the human aorta. The inner diameter of the ascending aorta and the three aortic arch branches were 35 and 8.5 mm, respectively. A

cannulation site of 10 mm in diameter was created at the outer wall of the ascending aorta at 4 cm proximal to the origin of the brachiocephalic artery.

The simulated perfusion circuit was prepared for the extracorporeal circulation (ECC). Water (temperature 22–24 °C) was perfused into the aortic model by a centrifugal pump (HPM-15, NIKKISO Co., Ltd., Tokyo, Japan) driven by a motor (HAP-21, NIKKISO Co., Ltd) through the aortic cannulas connected to the ascending aorta. The aortic model was set in a transparent glass tank filled with water to avoid refraction. The perfusate from the three arch branches and the descending aorta were separately drained into a water chamber. The perfusion rate was set at 4.0 L/min of steady flow. The perfusion pressure was maintained from 60 to 80 mmHg by compressing the circuit tube that collected the effluent from the three arch branches, using an occluder to control the circuit resistance. Perfusion pressure was monitored by a pressure monitor (DS-7210, DYNASCOPE, Fukuda Denshi Co., Ltd., Tokyo, Japan) that was connected to the arch branches.

Aortic cannulas

We compared the following two aortic cannulas in this study: Stealthflow 7.0 mm (TOYOBO 7.0 mm, TOYOBO Co., Ltd., Osaka, Japan); and Sarns Soft-flow model 5767, 7.0 mm (3 M Cardiovascular, Ann Arbor, MI, USA). The Stealthflow cannula has a pentagonal outlet with an obtuse angle, resulting in flame-like flow. The Soft-flow cannula has a flow separator on the cannula tip, resulting in a four- directional jet stream (Fig. 2).

Visualization of flow patterns

Particle image velocimetry (PIV) and high-speed video image analysis were used to analyze flow dynamics in the mock aortic model. The PIV system consisted of the fol- lowing four elements: a double-pulsed Nd:YAG laser system (Solo II-15, New Wave Research, Inc., Fremont, CA, USA), a cross-correlation camera (MEGAPLUS model ES1.0, REDLAKE MASD, Inc., Tucson, AZ, USA), a laserpulse synchronizer (LaserPulse, TSI, Inc., St. Paul, MN, USA), and PIV analysis software (Koncerto, SEIKA Co., Tokyo, Japan). High porous polymers (MCI GEL HP20P, Mitsubishi Chemical Co., Tokyo, Japan; diameter, 75–150 μm) were mixed in water as the tracer for the PIV system. As the quantity of polymer gel was small, we speculated its contribution to overall viscosity could be overlooked. A sheet-like formed double-pulsed laser (wavelength 532 nm; frequency of pulse 15 Hz; double pulse interval 500

μs; power 30 mJ) was emitted to the aortic arch model. The model was set in a water tank to visualize tracers reflected by the laser. A cross-correlation CCD camera (synchronized with a double-pulsed laser system) captured the images from the tracers. The movement of tracers in a 500 μs window was expressed as vectors in two directions (x- and y-axes) by the PIV analysis software. The degree of turbulence was calculated by a computer program and was expressed in the longitudinal flow map.

Flow image and velocity mapping

The velocity mapping and flow images by streamlines were constructed from mean velocity (U) and vectors from 30 to 50 consecutive images. Streamline and flow velocity were depicted in the longitudinal and short-axial planes. Distribution of flow velocity was depicted in a two-directional color map expressed with a color gradient from blue to red, ranging from 0 to [0.5 m/s, respectively. Short-axial flow patterns were taken along the greater curvature of the aortic arch.

Velocity mapping and flow images by streamlines were constructed from mean velocity (U) and directions of vectors of 30–80 consecutive images, as defined by the following equation:

$$U = \frac{1}{n}\sum_{i=1}^{n} u_i$$

Flow velocity vectors were taken at the longitudinal planes and axial planes perpendicular to the centerline of the aortic model. Flow vectors were analyzed in each axial plane. The longitudinal components of the flow vectors along the aortic axis are expressed in the histogram (Fig. 3).

Results

Stealthflow cannula

In the Stealthflow cannula, a high-velocity area with maximum velocity of 0.68 m/s appeared on the ostium of the cannula in the longitudinal plane. The main stream- trace was directed toward the lesser curvature side of the aortic arch, going toward the left subclavian artery (Fig. 4). Points 1-4 indicate the short-axial view of the ascending aorta, while points 5, 6, and 7 indicate the brachiocephalic artery, the left common carotid artery and the left subclavian artery, respectively. Flow velocity decelerated from 0.7 m/s at the axial view of point 4 (at the plane originating the proximal arch) on the lesser curvature to 0.5 m/s at the axial view of point 5 (at the plane originating the brachiocephalic artery) on the lesser curvature. The stream went down

along the lesser curvature of the aortic arch, making a single vortex. Although flow velocity varied widely, flow velocity around the ostia of arch vessels was slow (Fig. 5, solid line). Flow velocity was also slow in the ascending aorta. A large vortex of slow velocity and regurgitant direction was observed in the distal aortic arch around the subclavian artery in the longitudinal view. The vortex in the short-axial view was simple when compared with that associated with the Soft-flow cannula. Maximum forward flow was 0.68 m/s, appearing on the lesser curvature side, and that of regurgitant directed flow was -0.21m/s, appearing on the greater curvature side (Fig. 6).

Soft-flow cannula

With the Soft-flow cannula, multiple jet streams, each with a velocity less than 0.6 m/s, were observed at the cannula outlet (Fig. 4). One of the main streams went toward the posterior wall of the ascending aorta. A large regurgitant flow vortex was observed at the greater curvature side of the ascending aorta. The stream-trace was complicated, making small secondary vortexes in the ascending and the transverse aortic arch in the axial view (Fig. 4). Flow decelerated from 0.5 to 0.3 m/s between the opposite site of the brachiocephalic artery ostium (point 5) and that of the left common carotid artery ostium (point 6) (Fig. 5). Maximum forward

flow was 0.58 m/s, appearing on the lesser curvature side, and maximum regurgitant directed flow was - 0.27 m/s, appearing on the greater curvature side of the aortic arch (point 7).

Neck vessels flow properties

Flow velocity was measured at the orifice of each neck vessel. In the Stealthflow cannula, flow velocity on the ostium of the brachiocephalic artery, the left common carotid artery and the left subclavian artery was 0.133, 0.066 and 0.069 m/s, respectively. In the Soft-flow cannula, flow velocity on the ostium of these vessels was 0.118, 0.055 and 0.029 m/s, respectively. There is no backward, regurgitant flow from the neck vessels into the transverse aortic arch.

Discussion

Atheroembolism is a major cause of non-cardiac complications following open-heart surgery. Manipulation of the atherosclerotic aorta via aortic cannulation, application of the cross-clamp and the side-biting clamp may cause embolism of the atheromatous material into cerebral vessels, visceral arteries, and peripheral arteries. An autopsy study of cerebral pathology after CPB showed atheroembolism in 16.3 % of the brains [2]. In patients with a severe atheromatous aorta, the perfusion strategy is important, because jet flow-induced atheroembolism can occur in

the context of CPB [3, 4]. Cognitive damage after open-heart surgery may occur in up to three quarters of patients at the time of discharge from the hospital and in up to a third of patients after 6 months. The potential cause of atheroembolism lies in the jet emerging from the aortic cannula, which delivers oxygenated blood from the CPB directly to the aortic arch [5]. These emboli may eventually reach the brain through the aortic arch vessels [6, 7].

Dispersive-type aortic cannulas were developed to attenuate the jet flow from the arterial perfusion cannula. The Soft-flow arterial perfusion cannula was introduced in the early 1990s [8]. The concept of this cannula is to split flow into four streams via the four side holes and the cone- shape flow divider at the tip of the cannula. Dispersed streams have low kinetic energy and decelerate within several centimeters from the exit, thereby avoiding the sand-blast effect due to jet flow.

Our study conducted an experimental comparison of two cannulas. The jet stream was directed toward the lesser curvature of the aortic arch in both cannulas. Although flow velocity decreased gradually, flow velocity on the lesser curvature was high. Therefore, clinicians should be careful if frail atheroma exists on the lesser curvature of the aortic arch. Retrograde flow from the distal aortic arch into the left subclavian artery, as shown in the end-hole cannula [1],

was not observed with either cannulas. Flow velocity around the arch vessels was slow, especially with the Stealthflow cannula (Fig. 5, 6, 7). Flow velocity (0.1 m/s) was as slow as flow from the normal aortic orifice. Further, the counter-clockwise regurgitant flow from the cannula to the brachiocephalic artery to the ascending aorta on the greater curvature was specific to the Soft-flow cannula (Fig. 7). The degree of regurgitation at the same site was lower with the Stealthflow cannula than with the Slow-flow cannula (Fig. 6).

The Soft-flow cannula was recently withdrawn from market by the United States Food and Drug Administration. The Stealthflow cannula has the same flow dynamic property as the Soft-flow cannula. The advantage of Stealthflow cannula is the gentle flow pattern on the greater curvature of the aortic arch. In cases with thick, frail, and soft atheroma on the lesser curvature, an alternative method (such as a cannula tip directed toward the aortic root) should be considered.

Limitation of this study

This study had several limitations. First, our methodology may be too simplified to reflect clinical reality, as 22 °C water was used as the perfusate. As blood viscosity changes with

temperature and as the viscosity of water equals heparinized blood at a hematocrit less than 15 %, we tested a glycerin solution in a preliminary experiment, using a normal aortic arch model. The result was essentially the same as that when using water. We therefore used water as the perfusate to obtain an accurate comparative analysis. The Reynolds number, which influences the flow pattern in ‘‘laminar flow’’, was lower than that found in vivo. In this study, the Reynolds number for the jet stream at the cannula exit site was calculated as 14,400, which can be characterized as a ‘‘turbulent flow.’’ Although flow and strain patterns may change when using another perfusate, we think that vortices and streams do not vary as much as turbulence, in which flow does not transform into laminar flow.

Second, the site of cannula insertion and the direction of the cannulas may affect the result. When the cannula is placed more proximally in the ascending aorta, the jet from the cannula would hit directly on the ascending aortic wall, regardless of the cannula type, resulting in high shear stress on the aortic wall. When the cannula was placed more distally in the ascending aorta (proximal arch), the jet flow from cannula would hit the greater curvature of the aortic arch, generating high shear stress on the aortic wall.

This study is based upon experimental results from 2D- PIV measurements. To analyze our result three-dimensionally, we measured flow vectors in the longitudinal and short-axial planes. To facilitate an understanding of three-dimensional flow structure, flow velocity distribution, and streamline in short-axial plane is shown in Fig. 4. Absolute values of flow vectors in short-axial plane were measured and are depicted in Figs. 5, 6 and 7.

Conclusions

The Stealthflow cannula has flow properties that are similar to those of the Soft-flow cannula in a glass aortic model analysis. The Stealthflow cannula generates gentle flow in the aortic arch and slow flow around the ostia of the aortic arch vessels and is as effective as the Soft-flow cannula. Care must be taken when patients have thick atheromatous plaque or frail atheroma on the lesser curvature of the aortic arch.

Acknowledgments

We thank Masanori Ochi and Ryota Sakabe for their assistance with PIV analysis. This study was supported by JSPS KAKENHI Grant Number 24592044.

Compliance with ethical standards

Conflict of interest

Dr. Ikuo Fukuda is an inventor of the Stealth- flow cannula. All other authors declare that they have no conflicts of interest.

References

1. Minakawa M, Fukuda I, Yamazaki J, Fukui K, Yanaoka H, Inamura T. Effect of cannula shape on aortic wall and flow turbulence: hydrodynamic study during extracorporeal circulation in mock thoracic aorta. Artif Organs. 2007;31:880–6.

2. Blauth CI, Cosgrove DM, Webb BW, Ratliff NB, Boylan M, Piedmonte MR, Lytle BW, Loop FD. Atheroembolism from the ascending aorta. An emerging problem in cardiac surgery. J Thorac Cardiovasc Surg. 1992;103:1104–12.

3. Wareing TH, Davila-Roman VG, Barzilai B, Murphy SF, Kouchoukos NT. Management of the severely atherosclerotic ascending aorta during cardiac operations. J Thorac Cardiovasc Surg. 1992;103:453–62.

4. Ura M, Sakata R, Nakayama Y, Goto T. Ultrasonographic demonstration of manipulation-related aortic injuries after cardiac surgery. J Am Coll Cardiol. 2000;35:1303–10.

5. Fukuda I, Minakawa M, Fukui K, Taniguchi S, Daitoku K, Suzuki Y, et al. Breakdown of atheromatous plaque due to shear force from arterial perfusion cannula. Ann Thorac Surg. 2007;84:e17–8.

6. Van der Linden J, Hadjinikolaou L, Bergman P, Lindblom D. Postoperative stroke in cardiac surgery is related to the location and extent of atherosclerotic disease in the ascending aorta. J Am Coll Cardiol. 2001;38:131–5.

7. Weinstein GS. Left hemispheric strokes in coronary surgery: implications for end-hole aortic cannulas. Ann Thorac Surg. 2001;71:128–32.

8. Muehrcke DD, Cornhill JF, Thomas JD, Cosgrove DM. Flow characteristics of aortic cannulae. J Card Surg. 1995;10:514–9.

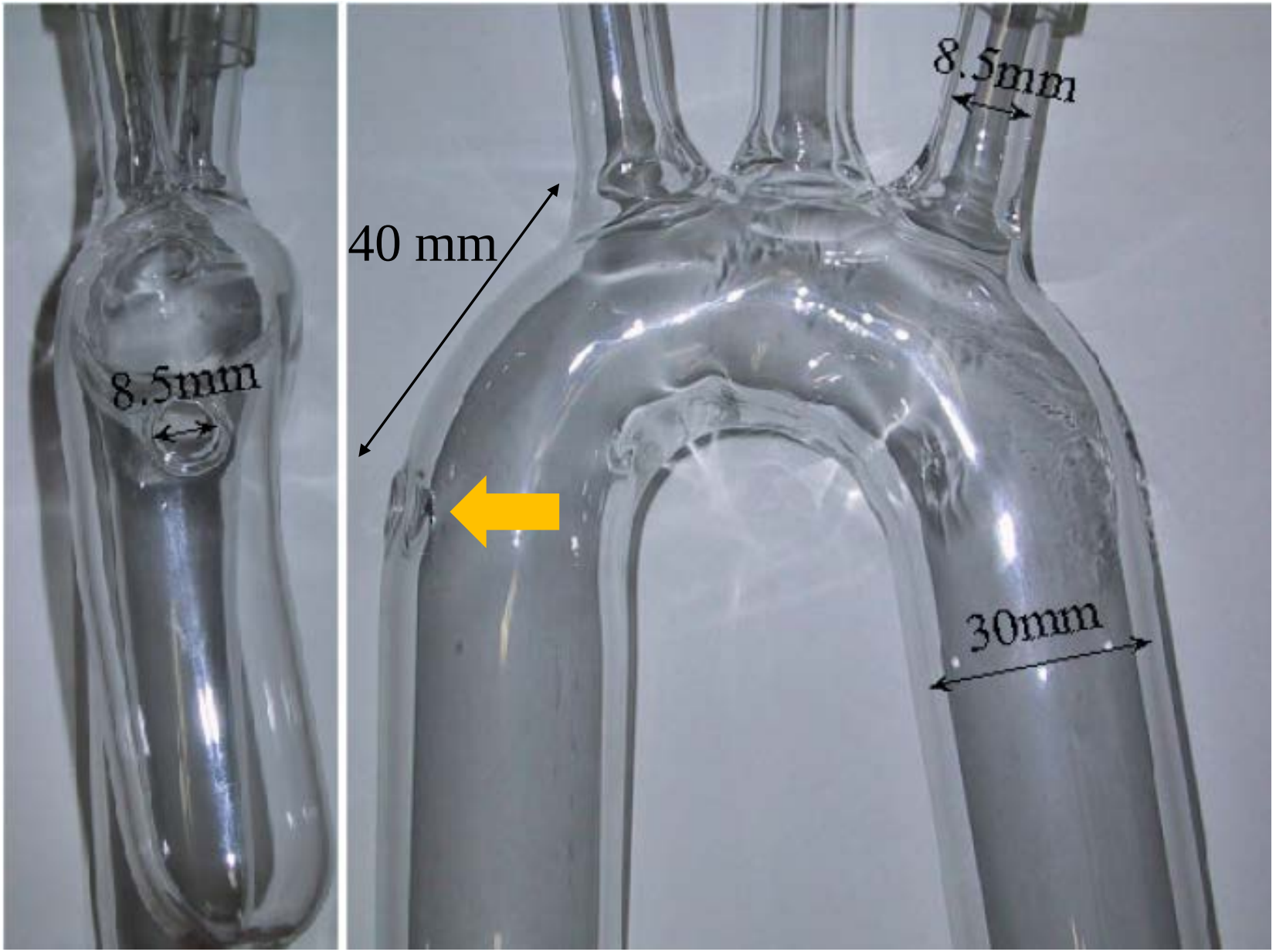

Fig. 1. The glass model of the aorta was constructed from a healthy adult.

A

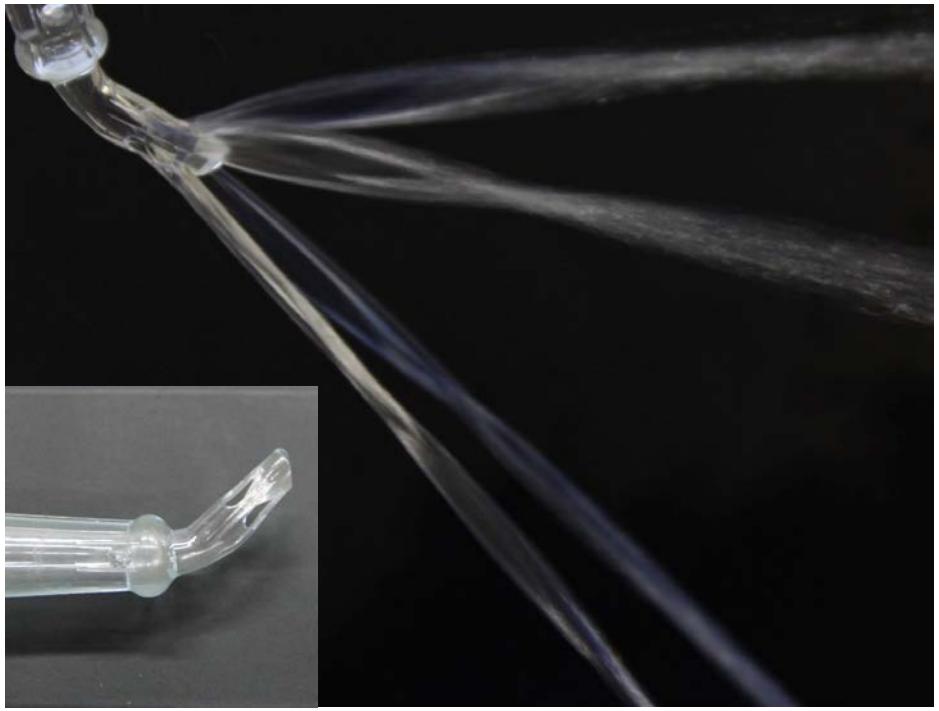

B

Fig. 2. Shape of cannula tip and jet-flow shape in open air. A: Stealthflow cannula, B: Soft-flow cannula.

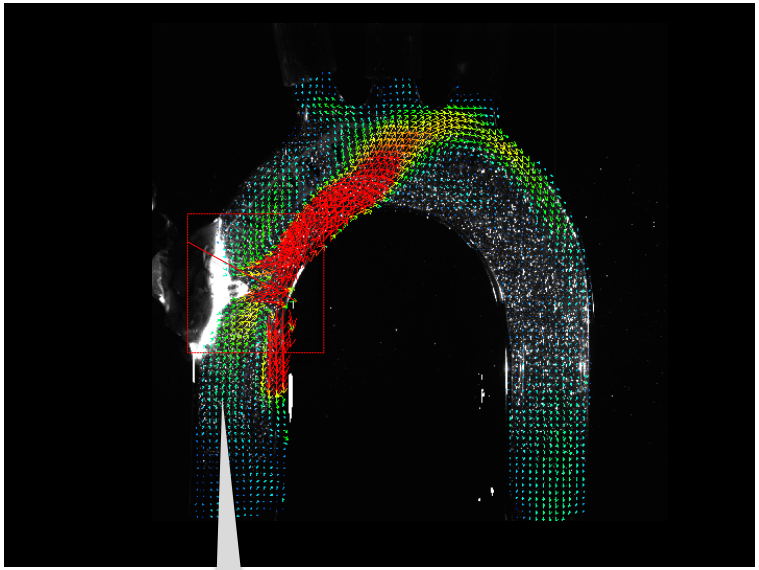

1

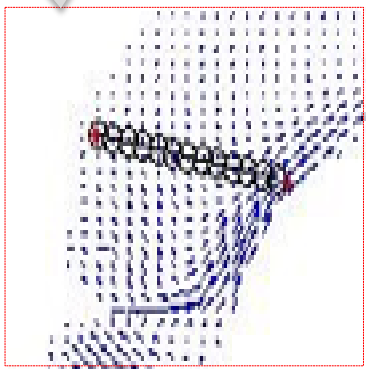

2

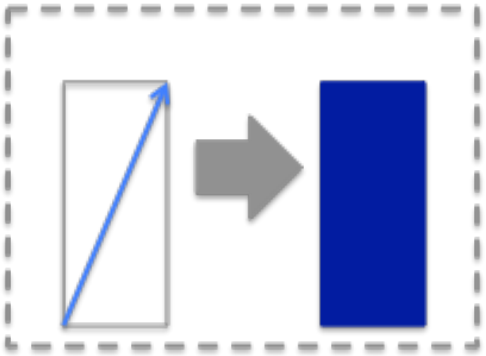

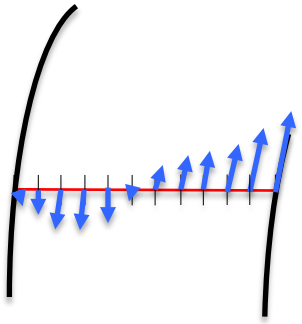

The greater curvature

The lesser curvature

3

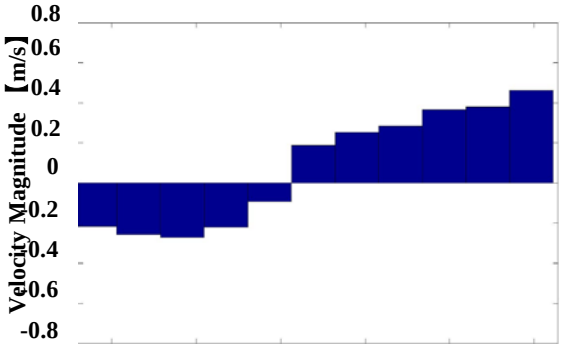

4

Fig. 3. Method for creating schematic drawing of velocity histogram.

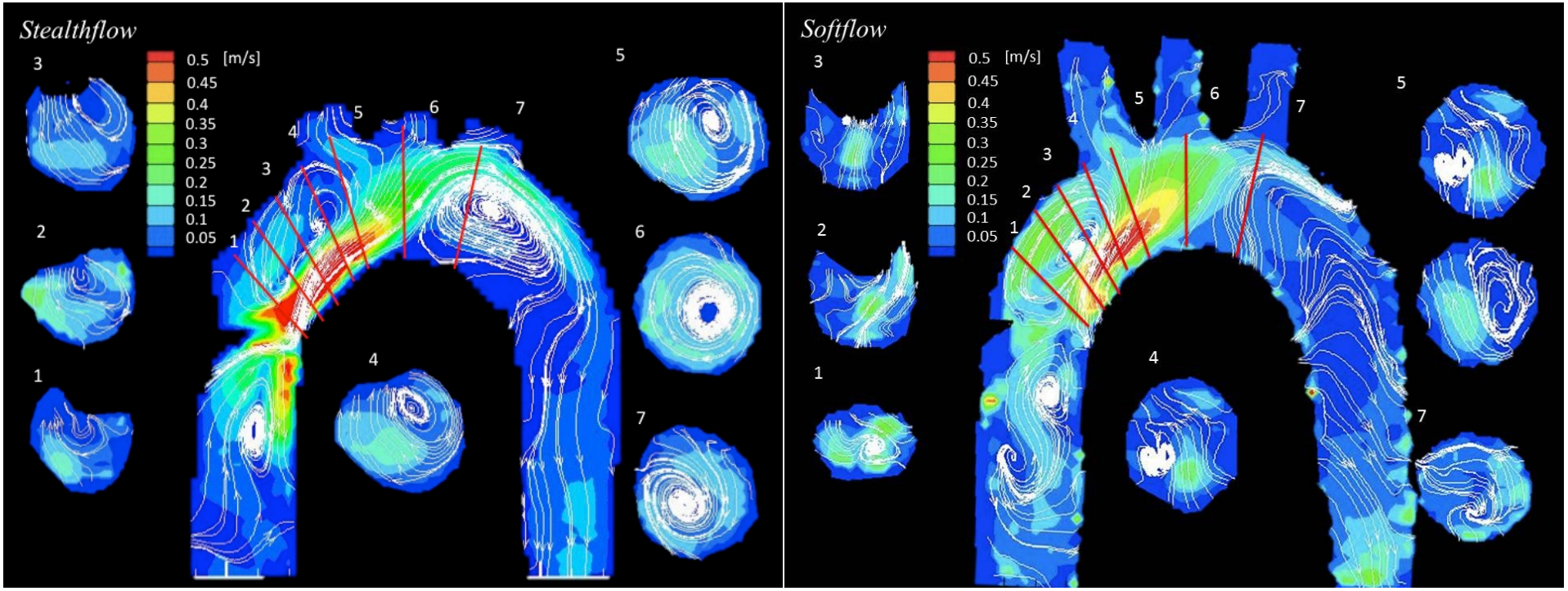

A *B*

Fig. 4. Flow velocity map in longitudinal section (center) and axial section (rims) for Stealthflow (A) and Soft-flow (B).

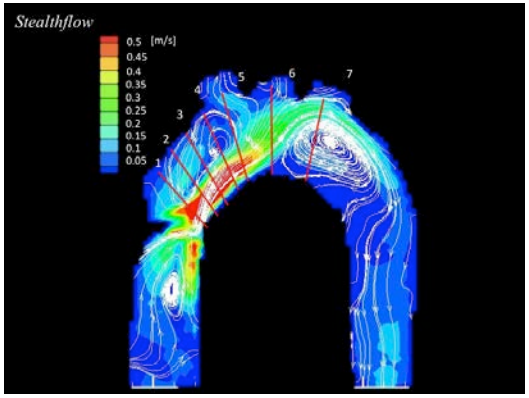

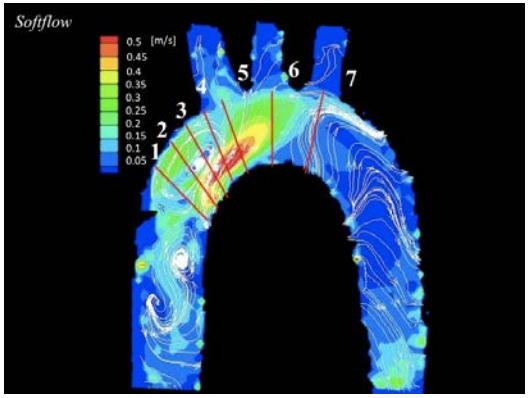

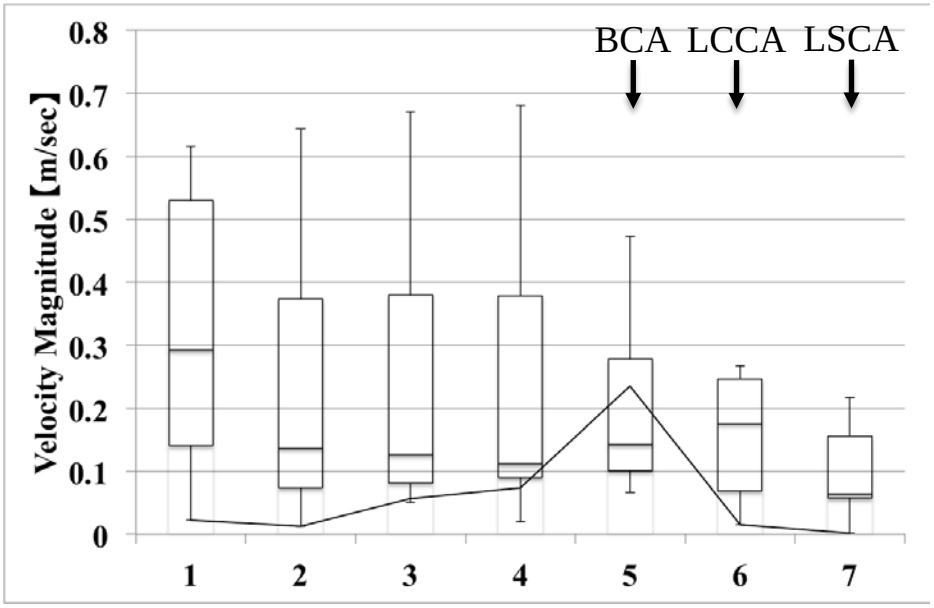

A

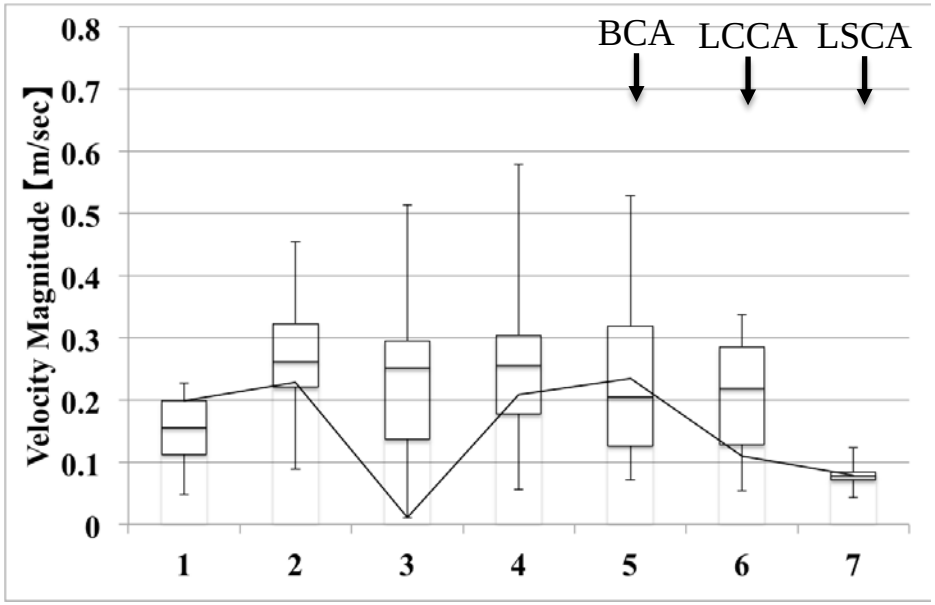

B

Fig. 5. Distribution of flow velocity (absolute value) plotted in each axial section. A) Stealthflow cannula, B) Soft-flow cannula.

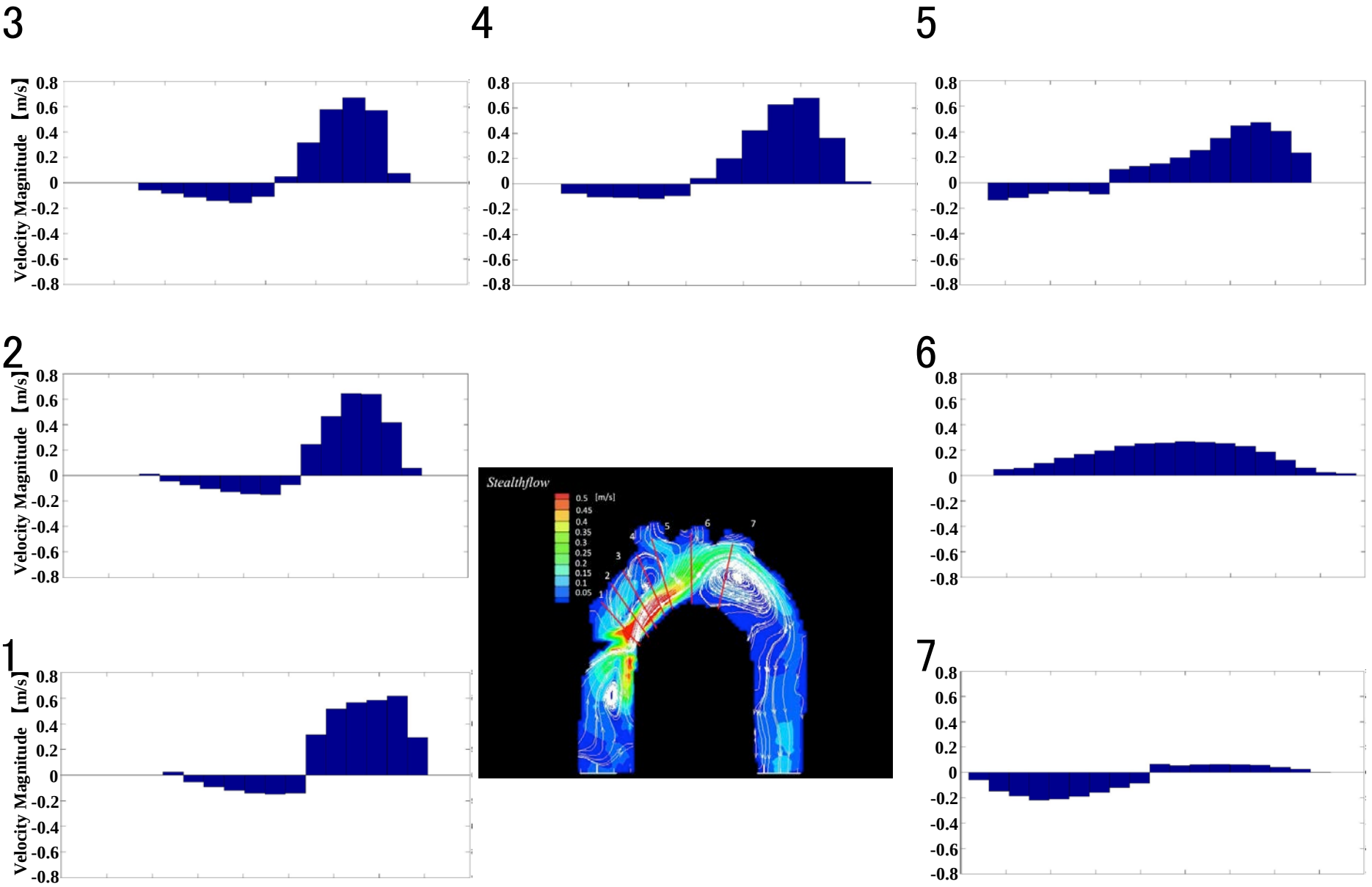

Fig. 6. Histogram of longitudinal flow components along the center of the aorta in each axial section in Stealthflow cannula.

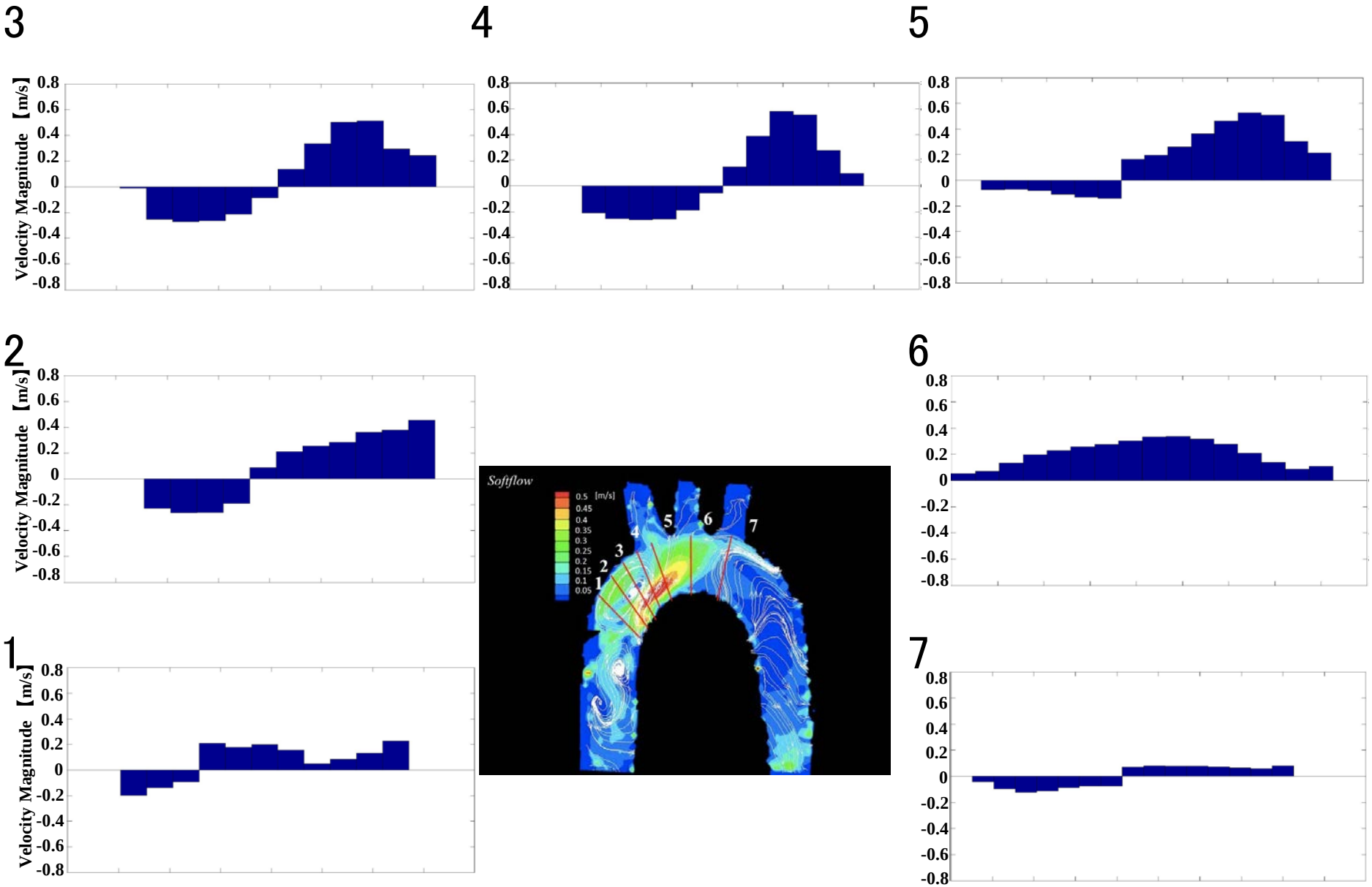

Fig. 7. Histogram of longitudinal flow components along the center of the aorta in each axial section in Soft-flow cannula.